A Simple Approach to Extract the Small Signal Model Circuit Elements for RTD

Eng.Rania M. Abdallah
Electrical Engineering Dept.
Fac. Of Engineering, Port Said University
Port Said, Egypt
eng_rania99@hotmail.com

Dr. Ahmed A. S. Dessouki
Electrical Engineering Dept.
Fac. Of Engineering, Port Said University
Port Said, Egypt
Dessouki2000@yahoo.com

Prof. Dr. Moustafa H. Aly
College of Engineering
Arab Academy for Science &Technology
&Maritime transport, Alexandria, Egypt.
Moustafa.Hassan@aast.edu, OSA member.

Abstract—**Most of Resonant Tunneling Diode (RTD) small signal model equivalent circuit elements extraction approaches are based on fitting the equivalent circuit model with measured S-parameter data over the frequency at certain bias points in the three regions of RTD current – voltage characteristics. In this paper, we propose a simple approach to extract widely employed RTD small signal model equivalent circuit elements. This approach is based on fitting the RTD DC analytical model with the measurement of the current – voltage characteristics of a given resonant tunneling diode in the entire bias range using a MATLAB routine. Then, the equivalent circuit elements (the quantum capacitance, quantum inductance and the conductance) are expressed as set of related analytical mathematical expressions as a function of the applied voltage. Simulation results show that the calculated equivalent circuit elements using the proposed approach exhibit a good agreement with measured data taken by another researcher for the same RTD structure in the entire bias range. In addition to, the proposed approach is easily incorporated into SPICE program to simulate the circuits containing RTD.**

Keywords- Resonant tunneling diode (RTD), small signal model, negative differential conductance, MATLAB, SPICE.

I. INTRODUCTION

The rapid progress in crystal growth and microfabrication technologies over the past two decades has led to the development of nanometer-scale semiconductor structures, where the wave-nature of electrons becomes relevant. As the size of a device scales down to that of an electron wavelength, quantum effects take over and new device concepts are needed beyond those used classically. Significant examples of such electronic components based on quantum effects are resonant tunneling diodes (RTDs) [1].

Resonant tunneling in semiconductor double potential barriers was first demonstrated by Chang, Esaki and Tsu in 1974 [2]. Since then, it has become a topic of great interest and was investigated both from the standpoints of quantum physics and of its application in functional quantum devices [1]. Over the past two decades, RTDs have received a great deal of attention.

RTDs have two distinct features when compared with other semiconductor devices, from an application point of view because of their potential for very high speed operation and their negative differential conductance (NDC) [1]. The former feature arises from the very small size of the resonant tunneling

structure along the direction of carrier transport. The NDC corresponds to an electric gain in active devices which can be applied in signal generation, detection and mixing, in multivalued logic switches at extremely high frequency, as well as in low-power amplifiers, local oscillators and frequency locking circuits [3, 4]. The RTD can also generate multiple high frequency harmonics, extending well into the submillimetre-wave band [1].

Most of RTD small signal model equivalent circuit elements extraction approaches [5-9] are based on fitting the equivalent circuit model with measured S-parameter data over the frequency at certain bias points in the three regions of RTD current – voltage characteristics or using a numerical analysis approach.

In this paper, we propose a simple approach to extract widely employed RTD device small signal model equivalent circuit elements (the quantum capacitance, quantum inductance and the conductance). This approach is based on fitting RTD DC analytical model with the measurement of the current – voltage characteristics of a given RTD in the entire bias range using a MATLAB routine. The parallel-inductance equivalent circuit [6,7], as shown in Fig. 1, and the RTD large signal model [10] have been employed to calculate the elements of the equivalent circuit model. To verify the results, the calculated elements of the equivalent circuit model are compared with the measurement data given in [7].

The rest of the paper is organized as following. In Section II, the equivalent circuit elements, shown in Fig. 1 and how to calculate each of them using the proposed approach have been presented. The simulation results and discussion are discussed in Section III. The paper is concluded in section IV.
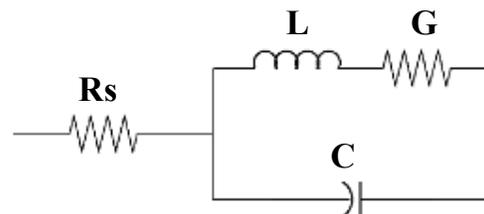

Fig. 1 Small signal equivalent circuit of RTD [7].

II. THE PROPOSED APPROACH TO CALCULATE THE EQUIVALENT CIRCUIT PARAMETERS

In this section, we discuss the equivalent circuit elements, shown in Fig. 1, in details and show how to calculate each of them using the proposed approach, where, the parallel-inductance equivalent circuit [6,7], as shown in Fig. 1, and the RTD large signal model [10] have been employed.

A. Conductance G

The equivalent circuit model includes a differential conductance G which is defined as

$$G = \frac{dI}{dV} \tag{1}$$

where I and V are the current and potential difference between adjacent bias points, respectively. Then, to get the conductance, numerically, one first uses MATLAB to accurately fit any real I-V characteristics and then numerically differentiate the computed I-V curve. From the described model in [10], the RTD I-V model is given by

$$I(V) = area \times \left(J_{exp}(V) + J_{Gaussian}(V) + J_{mod}(V) \right) \tag{2}$$

$$J_{exp}(V) = A(exp(B \times V) - exp(-B \times V)), \tag{3}$$

$$J_{Gaussian}(V) = C1\big(exp(-D1(V - E1)^2) \\ - exp(-D1(V + E1)^2)\big), \tag{4}$$

$$J_{mod}(V) = C2 \left(tan^{-1}\big(D2(V - E2)\big) \\ + tan^{-1}\big(D2(V + E2)\big) \right); \tag{5}$$

where A, B, C1, D1, and E1 are used to achieve different RTD I-V characteristics and are extracted using the parameters' extraction MATLAB routine. C2 controls the height of the added inverse tangent term. D2 controls the slope of this function, and consequently, can change the slope of the NDC. E2 controls the voltage of the middle point of the tangent function. Thus, it always has a value between the peak and valley voltages [10].

The derivative of the I-V curve is given by:

$$J'_{exp}(V) = AB(exp(B \times V) + exp(-B \times V)), \tag{6}$$

$$J'_{Gaussian}(V) = 2D1C1 \left(-(V - E1)\,exp(-D1(V - E1)^2) \\ + \big((V + E1)\,exp(-D1(V + E1)^2)\big) \right), \tag{7}$$

$$J'_{mod}(V) = C2 \left(\frac{D2}{1 + \big(D2(V - E2)\big)^2} \\ + \frac{D2}{1 + \big(D2(V + E2)\big)^2} \right); \tag{8}$$

and finally the differential conductance is calculated from

$$G = area \times \left(J'_{exp}(V) + J'_{Gaussian}(V) + J'_{mod}(V) \right). \tag{9}$$

B. Capacitance C

As listed above, the capacitance C, Fig.1, is defined as the summation of the geometrical depletion capacitance, Co, and the quantum capacitance, Cq, [9]

$$C = Co + Cq \tag{10}$$

where Co is defined as

$$Co = \frac{area}{\frac{LW}{\varepsilon w} + \frac{2LB}{\varepsilon p} + \frac{LD}{\varepsilon D}} \tag{11}$$

where LW is the width of the quantum well, LB is the width of the barrier, LD is the width of the depletion region, and εw, εp and εD are the dielectric constants of the quantum well, barrier, and depletion region, respectively [9].

The quantum capacitance, Cq, depends on the differential conductance and is given by [7,9,11]

$$Cq = -\tau_c \times G \tag{12}$$

where τ_c is the escape rate through the collector barrier.

C. Inductance L

The quantum inductance, L, in the equivalent circuit arises from the charge storage in the well [9]. It depends not only on the geometry of the device, but also on the scattering mechanism in the system. L can be expressed by the formula obtained by [6,7,9] as:

$$L = \frac{\tau}{G} \tag{13}$$

where the time constant, τ, is the electron lifetime which changes exponentially with the thickness of the barrier.

From the previous formula, it is noted that, the inductance L becomes negative in the NDC region due to the negative conductance.

The metal–semiconductor contact resistance, Rs, depends on the metal and material. A good result for metal semiconductor contact to InGaAs material is Rs = 5 Ω.

III. SIMULATION RESULTS AND DISCUSSION

A. Equivalent Circuit Parameters

In the proposed approach, we have endeavored to calculate the RTD small signal equivalent circuit parameters, G, L and C, as a function of the bias voltage and to compare the results to those of identical RTD measured by other researchers [7].

The geometrical capacitance Co, τ_c and τ used in Eqs. (11-13) are estimated by Qingmin et.al [7] to be: $Co = 29.3$ fF, $\tau_c = 0.79$ ps and $\tau = 2.58$ ps.

The device we have studied in this paper has an area of (1.6 X1.6 μm^2) and the RTD (I-V) characteristics exhibits a peak- to-valley current ratio (PVCR) of 2.02 with a peak current of $I_P = 2.69$ mA, peak voltage of $V_P = 0.312$ V and valley voltage of $V_V = 0.573$V, as shown in Fig.2 [7].

To extract device model parameters from the measured I–V characteristics, one needs first to obtain the fitting I–V characteristics.

Using the parameters' extraction MATLAB routine, the measured RTD I-V characteristic can be fitted to the model given in [10], as shown in Fig.2. The figure shows a good agreement between the measured (dashed line) RTD I-V curve [7] and the fitting (solid line) RTD I-V curve. The extracted model parameters are:

A= 3.6695 e+8 A/m2, B= 2.3545 V-1, C1= 8.1813 e+8 A/m2, D1= 10.5466 V-2, E1= 0.3427 V, C2= -4.9879e+8 A/m2, D2= 10.5470 V-1, E2 = 0.4018 V.

Fig.3 Comparison of the (line) calculated G with the measured (circles).

Fig.4. Reciprocal of the inductance L with a good agreement between the (circles) measured data and the calculated (line).
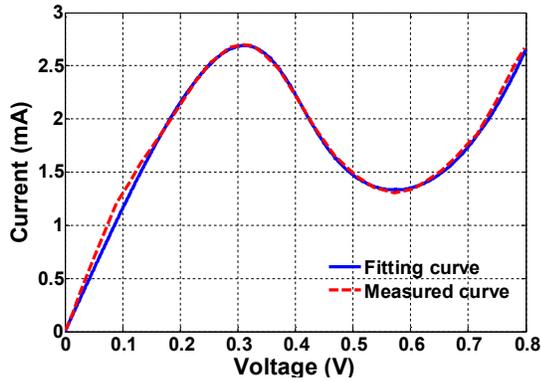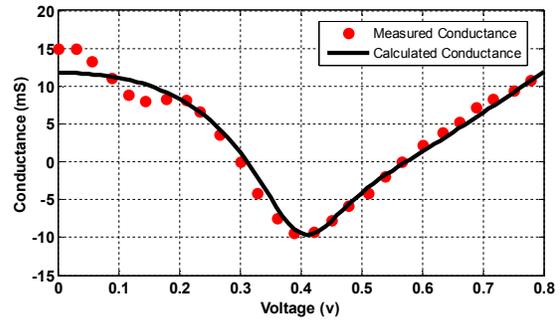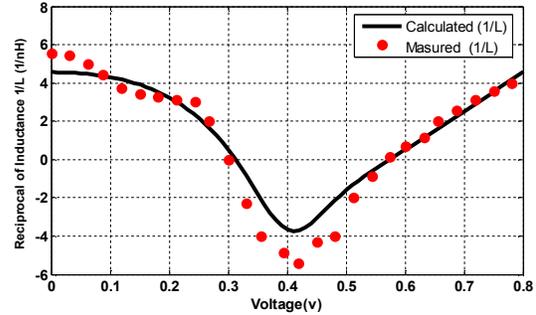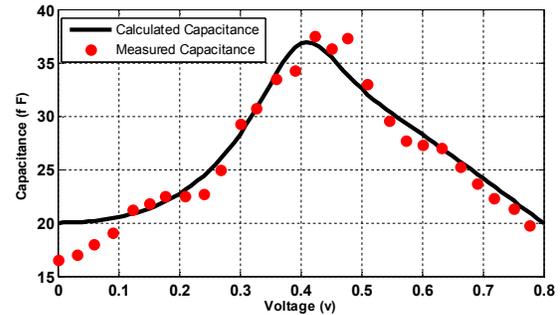

Fig.2 Comparison between the measured I-V RTD curve [7] and the RTD fitting I-V curve.

Using Eq. (9), one can calculate the differential conductance, G, as a function of the bias voltage as shown in Fig. 3. The figure shows a comparison between the calculated conductance using the proposed approach and the measured one [7]. A fair agreement between our calculated conductance and the measured data is obtained especially near the NDC region.

The quantum inductance, L, calculated from Eq. (13) is compared to that measured by Qingmin et.al [7] and a good agreement of the reciprocal of inductance L versus bias is shown in Fig.4.

Figure 5 compares the total capacitance, Eq. (10), and measured capacitance [7] showing a fair agreement between the calculated and measured data.

From the above figures, Figs. (3,4 and 5), it is concluded that, there are a fair agreements between the calculated values and measured data of the equivalent circuit elements (the quantum capacitance, quantum inductance and the conductance) at certain voltages. On the other hand, at other voltages, there are mismatches between the calculated values and the measured data due to the inaccuracy in the fitting process at these voltages.

Fig. 5. The capacitance C versus bias with close agreement between (circles) measured data and (line) calculation.

B. Calculation of Input Impedance

Figure 6 compares between the calculated input impedance using our simulation values (solid lines) of the quantum capacitance, quantum inductance and conductance and that calculated using the measured data (dashed lines) at various biases, i.e. V = 0 (inaccurate fitting point), V = 0.24 (accurate fitting point) in the first positive differential region, V = 0.54 (accurate fitting point) in the negative differential region and V = 0.75 (accurate fitting point) in the second positive differential region. The calculated input impedance of the equivalent circuit shown in Fig.1 can be expressed by:
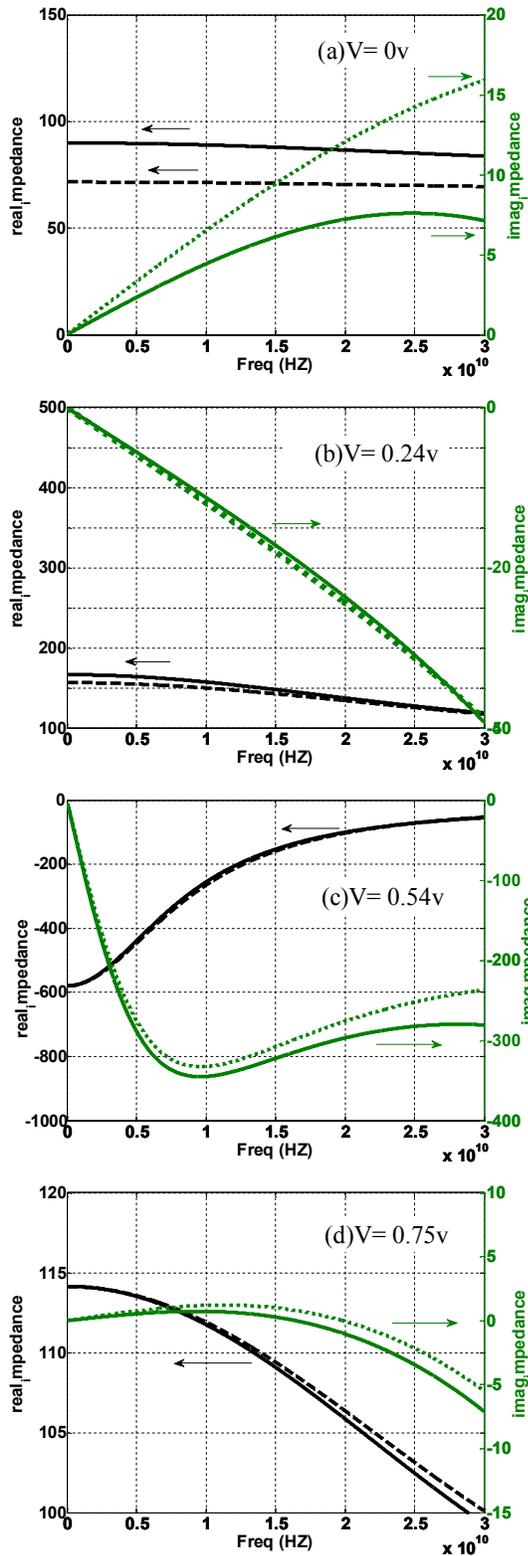
$$Z_{real} = Rs + \frac{R_D}{(1-\omega^2 CL)^2 + (\omega C R_D)^2} \qquad (14)$$

$$Z_{imag} = \frac{\omega L - \omega C R_D{}^2 - \omega^3 L^2 C}{(1 - \omega^2 CL)^2 + (\omega C R_D)^2} \qquad (15)$$

$$Z_{in} = Z_{real} + j Z_{imag} \qquad (16)$$

where ω is the angular frequency and RD is the inverse of conductance G.

It is concluded that, good agreements occur at the accurate fitting voltages and bad agreement at the inaccurate fitting voltage. So it is recommended to enhance the fitting accuracy, as much as possible, to get better results.

The proposed approach, also, allows us to calculate the equivalent circuit elements over the whole bias range in the three regions of RTD current and then the input impedance can be calculated over the entire frequency range and bias range as shown in Fig.7. This figure exhibits the real and imaginary values of the input impedance over the entire bias rang (0 to 0.8) volt and frequency range (45 MHz to 30GHz). Input impedance peaks are observed near the (I-V) peak and valley voltages.
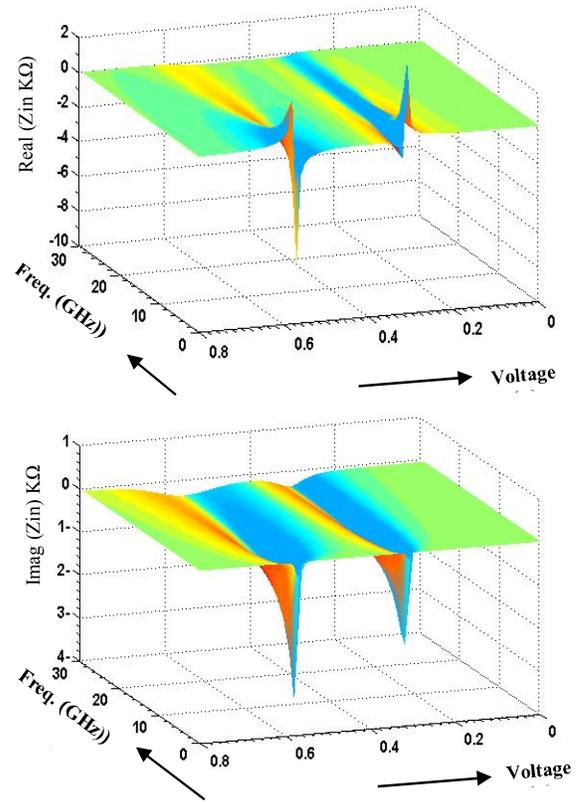

Fig.6 Real and imaginary of input impedance for the RTD at different voltages: (a) 0V, (b) 0.24V, (c) 0.54V and (d) 0.75V

Fig.7 Real and imaginary of input impedance over the entire frequency and voltage ranges.

V. CONCLUSION

In conclusion, a simple approach to extract widely employed RTD small signal model equivalent circuit elements is proposed. This approach is based on fitting RTD DC analytical model with the measurement of the current – voltage characteristics of a given RTD in the entire bias range. The equivalent circuit elements (the quantum capacitance, quantum inductance and the conductance) are expressed as set of related analytical mathematical expressions as a function of the applied voltage. Simulation results show that the calculated equivalent circuit elements using the proposed approach exhibit a good agreement with measured data taken by another researcher for the same RTD structure in the entire bias range. Also, input impedance can be calculated over the entire ranges of frequency and bias voltage. It has been observed that the accuracy of the results is dependent on the accuracy of the fitting process.

References

[1] Hiroshi Mizuta and Tomonori Tanoue, The physics and applications of resonant tunnelingca diodes, Cambridge University Press, Cambridge 1995.

[2] L. L. Chang, L. Esaki, and R. Tsu, "Resonant tunneling in semiconductor double barriers," Appl. Phys. Lett., vol. 24, no. 12, pp. 593-595, 15 June 1974.

[3] T. Akeyoshi, H. Matsuzaki, T. Itoh, T. Waho, J. Osaka and M. Yamamoto, "Applications of Resonant-Tunneling Diodes to High-Speed Digital ICs," Indium Phosphide and Related Materials Conference, Davos, 16-20, May, pp. 405 – 410, 1999.

[4] N. Muramatsu, H. Okazaki, and T. Waho, "A Novel Oscillation Circuit Using A Resonant-Tunneling Diode," IEEE International Symposium on Circuits and Systems, ISCAS, 23-26 May, pp. 2341-2344, vol. 3, 2005.

[5] A Zarea, A Sellai and M S Raven," Small signal analysis of resonant tunnel diodes in the bistable mode," 20th European Solid State Device Research Conference, ESSDERC '90 , Nottingham, England, 10-13 Sept, pp. 559-562,1990.

[6] E. R. Brown, C. D. Parker, and T. C. L. G. Sollner, "Effect of quasibound-state lifetime on the oscillation power of resonant tunneling diodes," Appl. Phys. Lett., vol. 54, pp. 934–936, Mar. 1989.

[7] Q. Liu, A. Seabaugh, P. Chahal, and F.J. Morris, "Unified AC Model for the Resonant Tunneling Diode," IEEE, vol. 51, no. 5, pp. 653-657, May 2004.

[8] P. Zhao, H. L. Cui, D. L. Woolard, K. L. Jensen, and F. A. Buot, "Equivalent Circuit Parameters of Resonant Tunneling Diodes Extracted from Self-Consistent Wigner-Poisson Simulation," IEEE, vol. 48, no. 4, pp. 614-627, April 2001.

[9] M A Long, H. Y. Long, Z. Yang, W. L. Chen, Y. F. Hua, Z. Y. Ping, "A Small Signal Equivalent Circuit Model For Resonant Tunneling Diode," Chin.Phys.Lett., vol.23, no.8, pp. 2292-2295, 2006.

[10] S.F.Nafea, A.A.S.Dessouki, "An accurate large-signal SPICE model for Resonant Tunneling Diode," International Conference on Microelectronics (ICM), Cairo, 19-22 Dec., pp.507-510, 2010.

[11] R. Lake and J. Yang, "A physics based model for the RTD quantum capacitance," IEEE Trans. Electron. Devices, vol. 50, pp. 785–789, Mar. 2003.